

Scale-Factor Corrections in Large Ring Lasers

B. Pritsch, K. U. Schreiber,* and A. Velikoseltsev

Technical University of Munich, Forschungseinrichtung Satellitengeodäsie

Fundamentalstation Wettzell, 93444 Bad Kötzing, Germany

J.-P. R. Wells

Department of Physics and Astronomy

University of Canterbury, Private Bag 4800, Christchurch 8020, New Zealand

(Dated: March 26, 2007)

Abstract

We report on fluctuations of the geometric scale factor of a very large ring laser situated thirty metres underground in the Cashmere Cavern in Christchurch (New Zealand). Variations in temperature and atmospheric pressure cause thermoelastic deformations to the cavern, which lead to changes of the area and perimeter of the ring laser structure. In-situ beam monitoring has been used to partially correct for these effects.

PACS numbers: 42.15.Dp, 42.30.Sy, 42.55.Lt, 91.10.Nj

*Also at Department of Physics and Astronomy, University of Canterbury, Christchurch, New Zealand;

Electronic address: schreiber@fs.wettzell.de

The past two decades have seen phenomenal progress in the development of large scale active Sagnac interferometers based on He-Ne gain media. Our previous efforts [7] have culminated in the development of the Gross-ring (G) in Wettzell (Germany), which encloses an area of 16 m² [6]. More recently, we have constructed very large scale ring lasers, ultra-G (UG) at the Cashmere Cavern in New Zealand. The UG1 ring has an approximately 20×20 m square cavity whilst UG2 has a rectangular design of approximately 20×40 m. The characteristics of the various ring lasers constructed in both Wettzell and Christchurch are given in table I. Two of the smaller instruments, namely C-II and G are fabricated in a monolithic structure, while all the other ring lasers are made from steel pipes placed on a number of small concrete piers on a cave floor. In particular the very large ring lasers UG1 and UG2 are subject to deformations of the Cashmere cave as a result of thermoelastic strain and atmospheric pressure variations.

Several mechanisms in a real world ring laser cause a departure of the actually measured Sagnac frequency from the theoretical value. In a much generalised form one can write

$$\Delta f = K_R(1 + K_A)\mathbf{n} \cdot \boldsymbol{\Omega} + \Delta f_0 + \Delta f_{bs}, \quad (1)$$

where $K_R = 4A/\lambda L$ is the geometrical scaling factor of an empty ring laser cavity. K_A accounts for the additional contributions due to the presence of an amplifying laser medium, while Δf_0 allows for mode pulling and pushing because of dispersion and Δf_{bs} takes the coupling of the two laser beams in the presence of backscatter into account [2]. These latter two effects are well established in the ring laser literature e.g. [1, 2] and are therefore excluded from the following discussion. Ring laser applications in Geodesy and Geophysics require ultimately stable and highly sensitive sensors [5, 6] with a demand for a relative sensor resolution of $\Delta\Omega/\Omega_E < 10^{-9}$.

The beat frequency obtained from a ring laser gyro is proportional to the scaling factor, the rotational velocity and the orientation of the area normal vector and the vector of rotation as shown in equation 1. However the normal vector of the area circumscribed by the laser beams is only well defined for a triangular ring. Since most of the very large ring lasers existing to date have a square or rectangular shape one needs to modify the definition of orientation for these instruments. Figure 1(a) outlines the procedure. Let us assume a square ring laser which is completely planar along the corners $ABCD$. Then the normal vector \vec{n} represents the entire area. If however one corner (C^*) is slightly tilted out of plane,

the effective area is obtained by subdividing the full area into triangles and projecting the normal vector \vec{n}_i of each subarea onto the rotation vector.

All the large ring lasers mentioned in Table I are placed horizontally on the Earth. Therefore they show a strong latitude dependence for the projection of the effective ring laser normal vector onto the Earth rotation vector of $\Omega_{eff} = \sin(\phi + \delta_N)$, with ϕ corresponding to the latitude of the instrumental site and δ_N representing a tilt towards North. East-west tilts are nearly negligible, since the cosine of an angle representing a small tilt towards East $\delta_E \approx 0$ is so close to 1 that it can be neglected, except for strong seismic motions.

For UG2, four highly reflecting supermirrors, placed on concrete foundations in the corner of the Cashmere cave form a rectangular laser cavity. Due to the long trajectories of 39.703 and 21.015 m in the laser arms, small mirror tilts in the range of a few seconds of arc cause a noticeable beam displacement on the next mirrors. As this corresponds to a change in the geometric scale factor, the beam walk was monitored and the instantaneous area and ring laser orientation (relative to the ring laser hardware structure) was computed. By placing a CCD camera next to the corner boxes enclosing the mirrors and recording the transmitting part of the laser beam, geometrical beam-walks at the level of one micron in displacement could be obtained. Figure 1(b) shows a representative example of the movement of the beam spot center position of several tens of microns with time, suggesting scale factor variations well above the desired level of 10^{-9} .

After the alignment of the UG2 ring laser, the cavity was refilled with a clean supply of helium and neon. A measurement sequence of approximately 2 weeks was started on Dec. 30, 2005 and lasted until Jan. 15, 2006. The Sagnac frequency was recorded with an integration time of 30 minutes. Figure 2(a) shows the measurement sequence as recorded on the logging system. Since UG2 is rigidly attached to the cave floor, one would expect Earth rotation to produce a constant Sagnac frequency with a stability at the 1 mHz level. However the measurements show an overall downward trend and superimposed systematic excursions of considerable amplitude, where some occur abruptly whilst others are more gradual.

From the instantaneous beam positions recorded by the cameras the geometrical variation in area and perimeter can be computed. It is found that the area is changing at the parts per million level. These fluctuations are correlated with the measured atmospheric pressure inside the cavern and it can be concluded that pressure induced deformations of the cave

are causing small tilts at the mirror mounts, which in turn cause beam walk on the next mirror. Similar results are obtained for the instantaneous orientation of the UG2 ring laser although these are much smaller than the variations in area, where a small tilt in the pointing angle amounts to comparatively large change in area. The perimeter changes inferred from ray-tracing based on the measured beam wander are approximately 6 orders of magnitude smaller. This is compatible with the general observation that the longitudinal mode index changes are infrequent. Finally the instantaneous geometrical scale factor was computed as a function of time for the entire period of the measurements with changes that amount to several parts per million for the UG2 ring laser. Similar measurements on the monolithically constructed G ring laser suggest that the scale factor variations from beamwalk are at least 2 orders of magnitude smaller and outside the range of resolution of the cameras. With all the geometric scale factor corrections applied, the timeseries of the measured Earth rotation rate smoothes out as shown in fig. 2(b). Apart from a major disruption around day 13 there is only a systematic downward drift of the form $-e^t$ left in the data set. The existence of such a distinct systematic feature suggests the presence of an independent influence on the optical frequencies in a ring laser cavity.

The residual downward trend is due to contamination of the laser gas with hydrogen, oxygen, nitrogen and water vapor via outgassing from the cavity enclosure and gives rise to an additional loss factor in the gain medium. This effect has been observed in a different context for linear HeNe lasers by [3] and [4]. UG2 with a stainless steel tube enclosing the laser gas along the entire perimeter of 121.435 m experiences a substantial amount of outgassing. On two occasions measurements of the total gas pressure inside the cavity were made, each over a period of 56 days. We observed an overall increase of 0.022 mbar and 0.020 mbar of hydrogen, amounting to 4×10^{-4} mbar H_2 per day taking the UG2 ring laser well into the regime where additional losses from absorption effects by hydrogen become visible. Because of the need to adjust our large ring lasers to single longitudinal mode operation near laser threshold, we are using a feedback circuit that stabilizes the gain medium to constant beam power. Increasing losses in the laser cavity therefore will raise the loop gain accordingly. We follow the approach of [1] K_A describes the contribution of the active medium to the scale factor of a large ring laser gyro as

$$\frac{\Delta K_A}{K_A} = \left(\frac{\Delta K}{K} \right)_N - \frac{aG}{1 + xP_o} + NL(\Omega). \quad (2)$$

In this equation $\Delta K_A/K_A$ corresponds to the scale factor correction due to the active laser medium, $(\Delta K/K)_N$ is the constant part of the scale factor correction, the second term on the right side allows for laser gain related contributions and the last term accounts for non linear contributions such as backscatter related coupling, which we neglect from the following discussion. Usually the gain factor G is considered constant with respect to time in ring laser theory. However for the reasons outlined above we account for the progressive compensation of gas impurity related losses by setting

$$G = G_0 e^{\alpha t}. \quad (3)$$

This choice is arbitrary and is motivated from the behavior of the loss in [3]. The beam output power of eq. 2 in the required form for large ring lasers with an isotope mixture of ^{20}Ne and ^{22}Ne becomes

$$P_o = 2I_s A_b T \left(\frac{G}{\mu} \cdot \frac{\kappa_1 Z_i(\xi_1) + \kappa_2 Z_i(\xi_2)}{Z_i(0)} - 1 \right), \quad (4)$$

with I_s the saturation intensity, A_b the beam cross section and T the transmission of the laser mirrors. Z_i is the imaginary part of the plasma dispersion function with lasing at a frequency detuning of ξ_n with respect to the respective line centers of the two Neon isotopes with each having a partial pressure of $\kappa_{1,2}$. The most important part in this equation is the factor $\frac{G}{\mu}$, which represents the gain – loss ratio. This factor is approximately constant over the time of the measurements because of the feedback loop operation. Since there is no drift in the optical frequency involved, the contribution of the plasma dispersion function also remains constant. Therefore the denominator in eq. 2 can be approximated to $1 + xP_o \cong 1$ so that this equation reduces to

$$\frac{\Delta K_A}{K_A} = \left(\frac{\Delta K}{K} \right)_N - aG_0 e^{\alpha t}. \quad (5)$$

Applied to the dataset of fig. 2b we obtain a corrected dataset as shown in fig. 2c after a nonlinear least squares fitting procedure.

In summary, we have measured, and partially corrected for, laser beam walk in a large scale active ring laser interferometer – UG2. Excellent results are obtained for the reduction of geometric scale factor variations, notwithstanding a gain medium related contribution to the scale factor caused by a gradual reduction in intra-cavity power related to contamination due to hydrogen outgassing.

Acknowledgments

This work was supported by the Bundesamt für Kartographie und Geodäsie (Germany) and through the Marsden fund of the Royal Society of New Zealand, research contract UOC106. We thank Dr. R. Hurst for his contributions and discussions, Dr. W. Schlüter for his support and Mr R. Thirkettle for technical assistance.

-
- [1] Aronowitz, F. (1999), Optical Gyros and their Application, RTO AGARDograph 339
 - [2] Wilkinson, J. R. (1987), Prog. Quant. Electr. Vol. 11, 1–103
 - [3] Hochuli, U. E., Haldemann, P., Li, H. A. (1974), Rev. Sci. Instrum., Vol. 45, No. 11
 - [4] Ahearn, W. E., Horstmann, R. E. (1979), IBM J. Res. Develop. Vol. 23, No. 2
 - [5] Schreiber K. U., Stedman G. E. and Klügel T.; J. Geophys. Res. **108** (B)2, 10.1029/2001JB000569
 - [6] Schreiber, K. U., Velikoseltsev, A., Rothacher, M., Klügel, T., Stedman, G.E., Wiltshire, D.L.; J. Geophys. Res. Vol. 109 No. B6, 10.1029/2003JB002803, B06405, (2004)
 - [7] Stedman, G. E. (1997); Rep. Progr. Phys. 60:615–688

TABLE I: Summary of physical properties of a number of large ring lasers

Ring Laser	Area, m^2	Perimeter, m	f_{Sagnac} , Hz	$\Delta\Omega/\Omega_E$
C-II	1	4	79.4	1×10^{-7}
GEOsensor	2.56	6.4	102.6	1×10^{-7}
G	16	16	348.6	1×10^{-8}
UG1	366.83	76.93	1512.8	3×10^{-8}
UG2	834.34	121.435	2177.1	5×10^{-8}

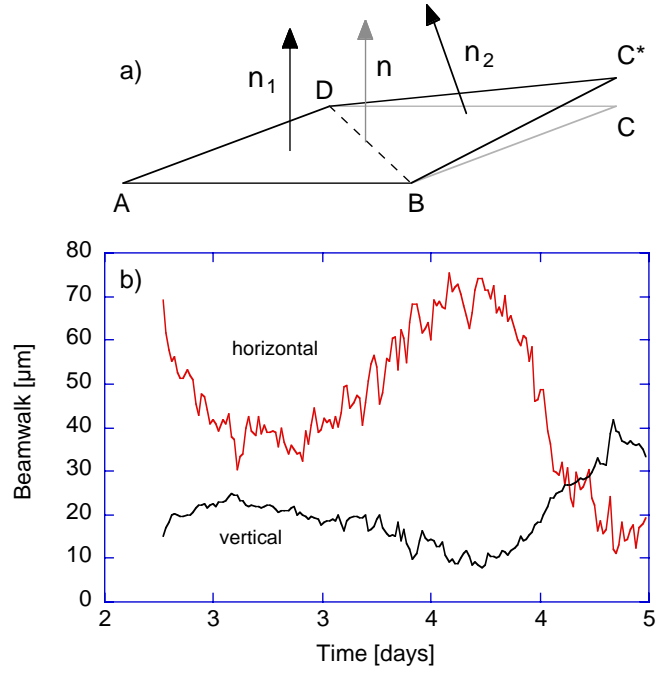


FIG. 1: The sum over the projection of the triangular subareas onto the axis of rotation define the effective ring laser normal a). The diagram shown in b) represent the observed beam wander over a measurement sequence of several days.

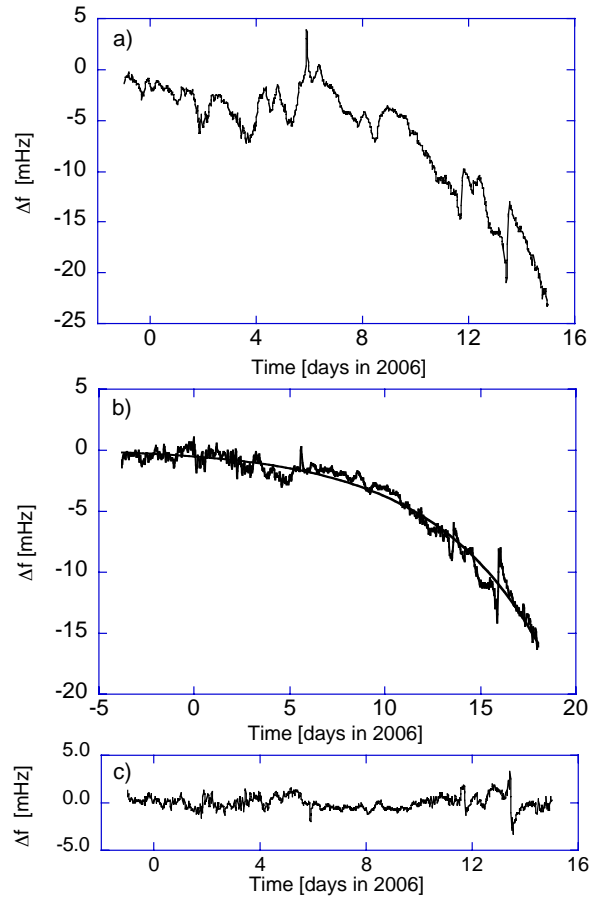


FIG. 2: Time-series of the Sagnac frequency caused by Earth rotation, monitored with the UG2 gyroscope. Raw data a), after the geometric scale factor corrections b) and after the reduction of the gain medium contribution c).